Использование супрамолекулярных систем для моделирования биологических процессов

Природные и искусственные ионофоры

Ионофоры - рецепторы, образующие устойчивые липофильные комплексы с заряженными гидрофильными частицами и способные переносить их в гидрофобную фазу (природная или искусственная мембрана).

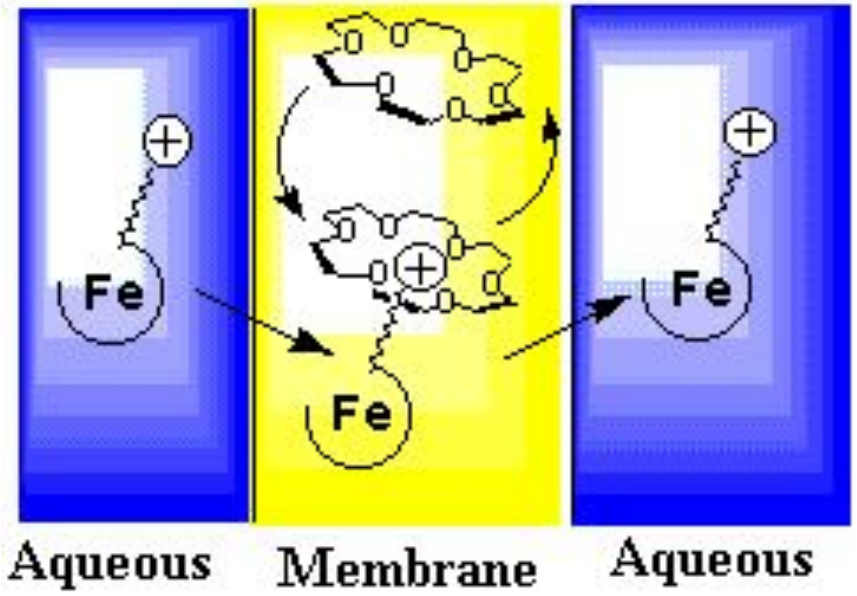

Валиномицин

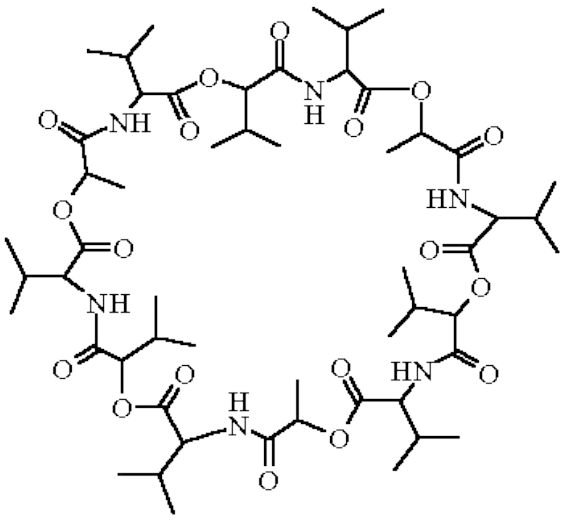

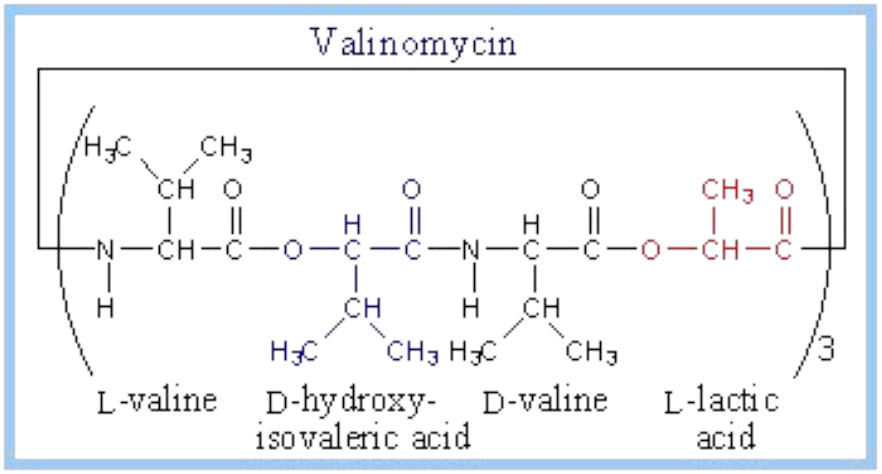

12 фрагментов окси- и аминокислот;
водородные связи **RNH--O=COR**

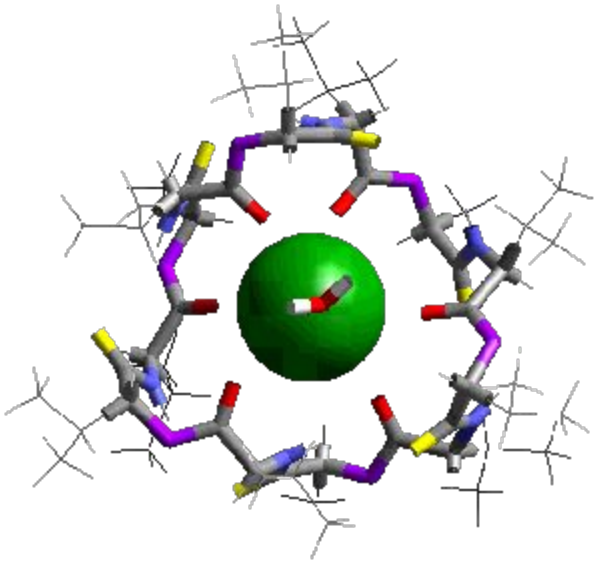

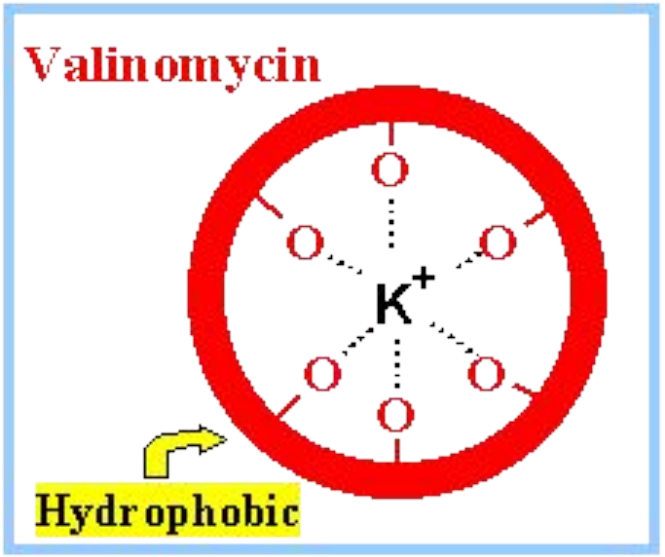

Боверицин

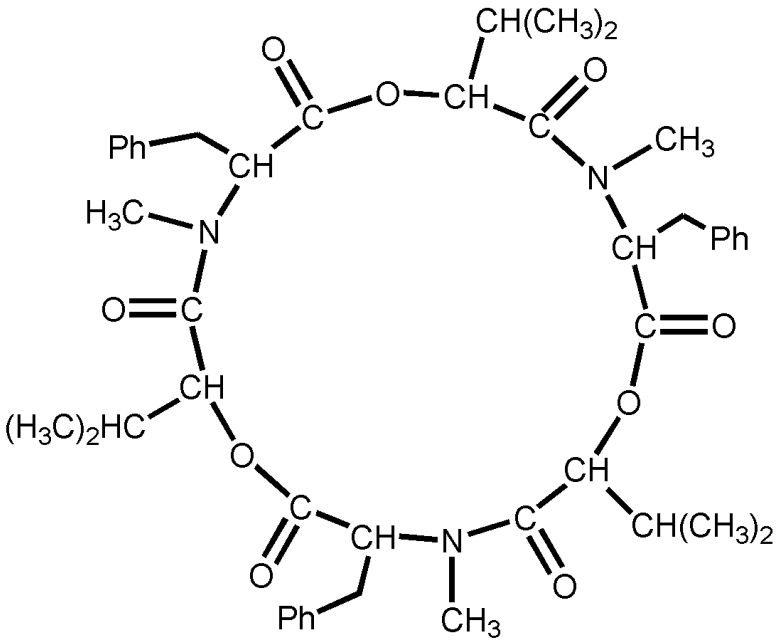

18-членный макроцикл

Комплекс димерной структуры $(BvBaPc_3BaBv)^+Pc^-$

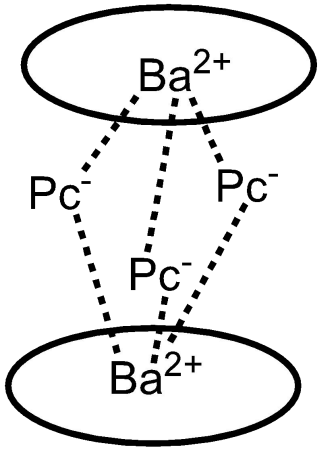

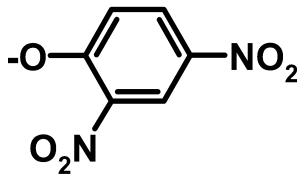

Циклические 32-членные тетралактоны

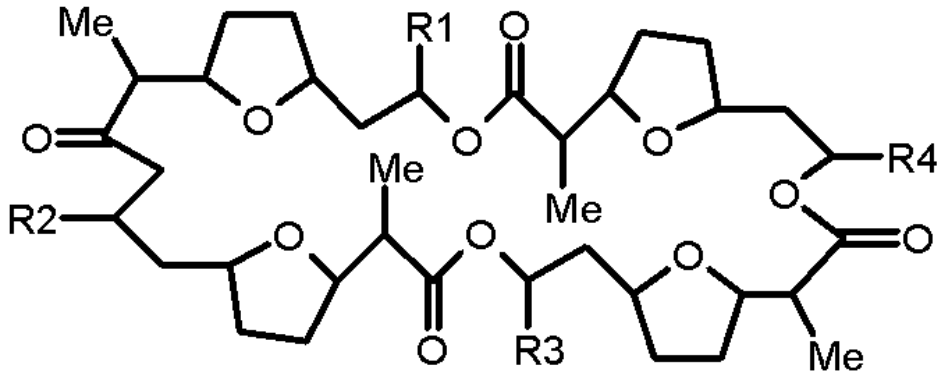

R^1 , R^2 , R^3 , R^4 = Me, Et
нонантин
монактин
динактин
тринактин
тетранактин

Прочные и селективные комплексы
с катионами щелочных металлов при переносе
через биологические и искусственные мембраны

-Координация катионов происходит по центру макроцикла
- Конформационная пересртойка при комплексообразовании
- Гидрофобная внешняя оболочка и гидрофильная внутреняя

Полиэфирные линейные антибиотики

Содержат:
концевые карбоксильную и гидроксильну группы;
несколько простых эфирных групп;
тетрагидрофуран или тетрагидропиран

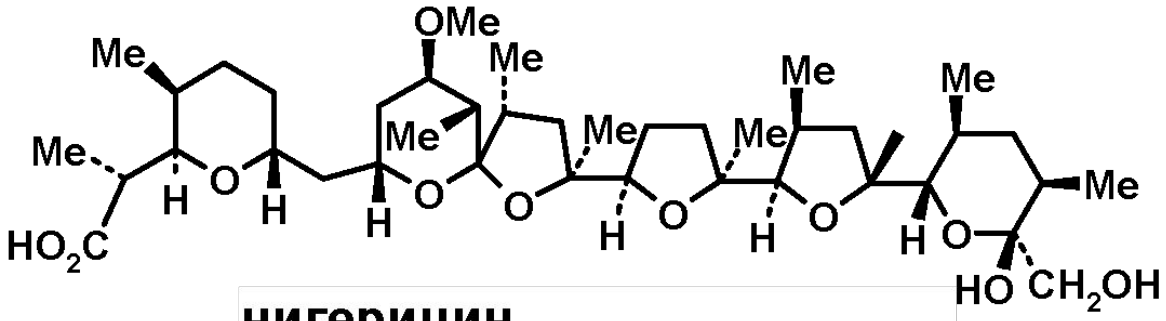

нигерицин
одновалентный
антибиотик

$K^+ > Rb^+ > Na^+ > Cs^+ > Li^+$

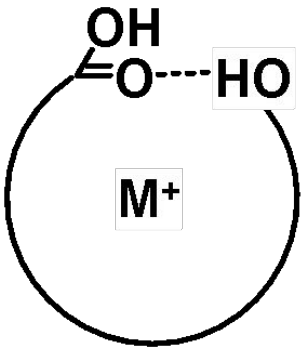

Комплексообразование

Двухвалентные антибиотики

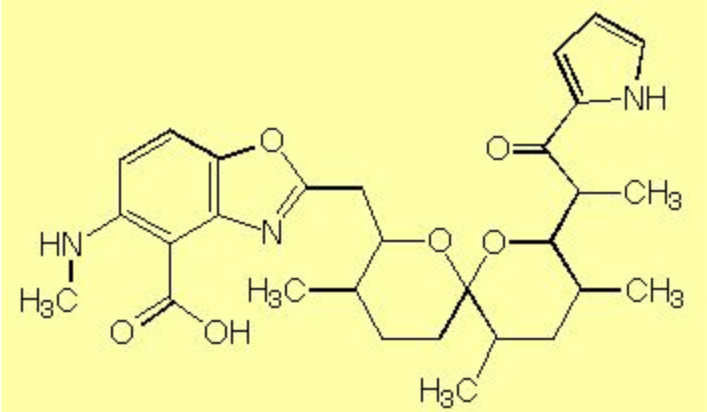

Calcium ionophore A23187

$RCOO-(Ca^{2}+)-OOCR$

Ca^{2+}----- $2H^{+}$

$Mn^{2+}>Ca^{2+}=Mg^{2+}>>Sr^{2+}>Ba^{2}$

Использование супрамолекулярных систем для моделирования биологических процессов

- **Разработка методов детекции аминов, карбоновых кислот и аминокислот, пептидов.**
- **Разработка методов введения флуоресцентных меток, других типов маркеров в ДНК.**
- **Разработка методов селективного разрушения молекул ДНК.**
- **Изучение мембранного транспорта органических молекул и катионов металлов.**
- **Искусственные каталитические системы.**

ЯМР-анализ стереоизомеров

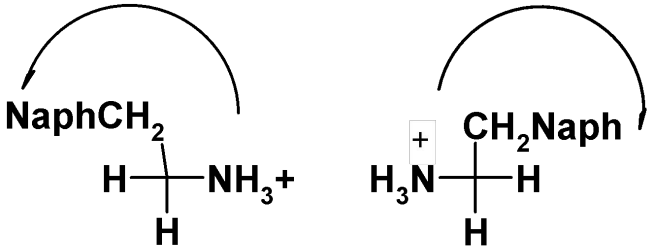

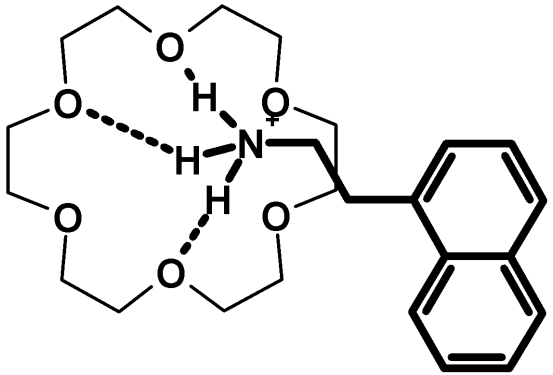

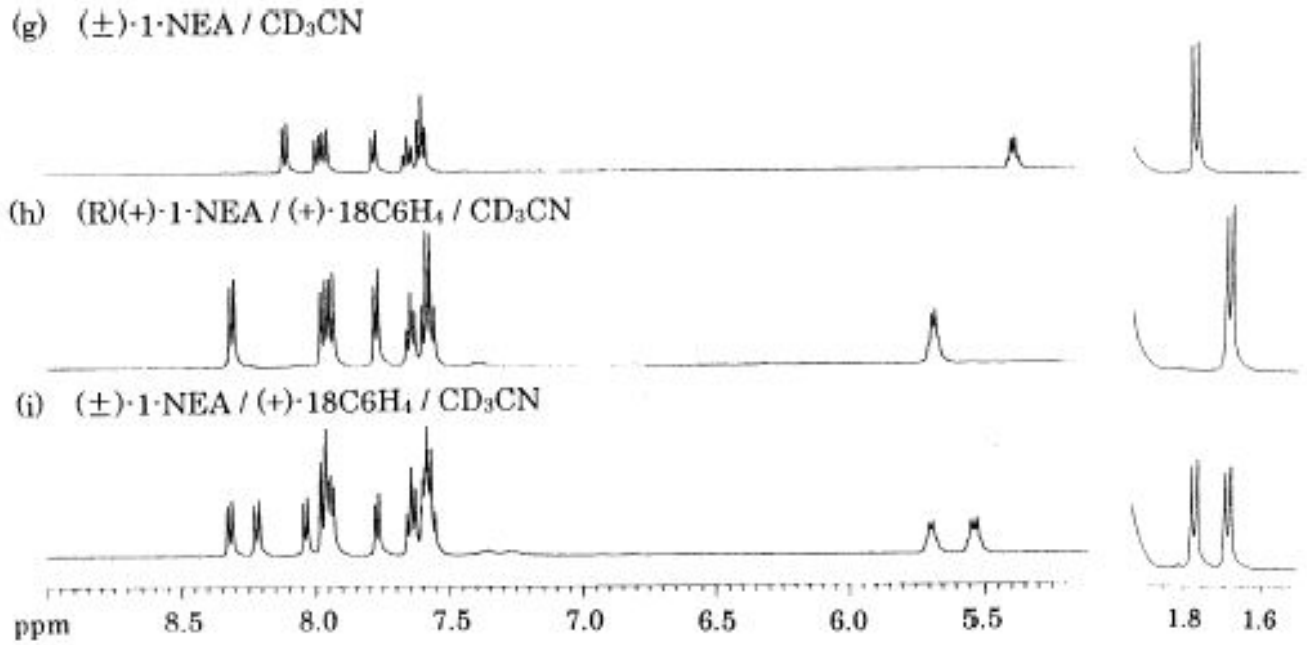

ЯМР-анализ стереоизомеров

Table 1
Effect of deuteration solvents on chemical shift change (R^1R^2–CH–NH_2)

Entry	Compounds R^1, R^2	Solvent	CH proton without 18C6H4	Δδ (CH proton with 18C6H4)	CH_3 proton without 18C6H4	Δδ (CH_3 proton with 18C6H4)
1	Phenylglycine (PheG) C_6H_5, COOH	D_2O	5.21	+0.07(L), +0.17(D)	–	–
2		CD_3OD	5.08	+0.38(L), +0.50(D)	–	–
3		CD_3CN	5.11	+0.20(L), +0.42(D)	–	–
4	1-Phenyethyl amine, (1-PEA) C_6H_5, CH_3	D_2O	4.54	+0.05(*S*), +0.03(*R*)	1.64	±0.00
5		CD_3OD	4.45	+0.29(*R*), +0.33(*S*)	1.63	−0.02(*S*), +0.06(*R*)
6		CD_3CN	4.50	+0.09(*R*), +0.16(*S*)	1.64	−0.03(*S*), ±0.00(*R*)
7	Alanine-β-Naphthylamide (Ala-β-NA) $C_{10}H_7NHCO$, CH_3	D_2O	4.30	+0.04	1.68	+0.00(L), +0.01(D)
8		CD_3OD	4.17	+0.15(D), +0.32(L)	1.65	−0.03(L), +0.06(D)
9		CD_3CN	4.34	Overlapped	1.66	−0.02(L), ±0.00 (D)
10	1-(1-Naphthyl) ethylamine (1-NEA) $C_{10}H_7$, CH_3	D_2O	5.46	+0.01(*S*), +0.09(*R*)	1.78	−0.02(*R*), +0.01(*S*)
11		CD_3OD	5.39	+0.21(*S*), +0.47(*R*)	1.76	−0.06(*R*), ±0.00(*S*)
12		CD_3CN	5.39	+0.14(*S*), +0.30(*R*)	1.77	−0.08(*R*), ±0.00(*S*)

All chemical shifts reported in ppm relative to TPS at 27 °C.

Оптический анализ стереоизомеров

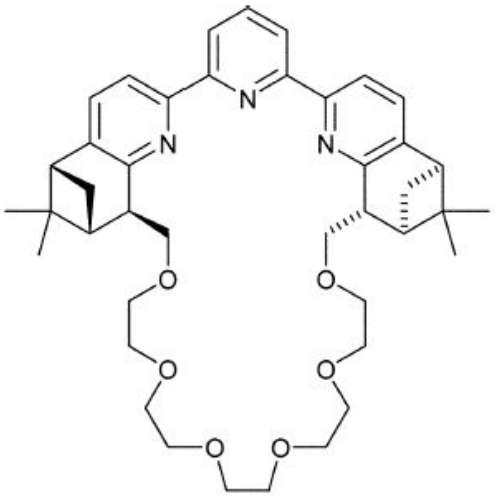

1

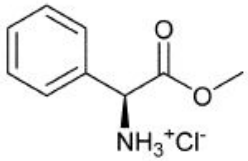

(*S*)-PhEtOMe

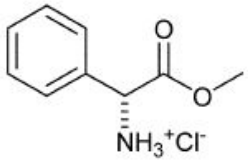

(*R*)-PhEtOMe

(4.2 ×10^{10} for the (*S*)- and
1.1 × 10^{10}M $^{-2}$ and (*R*)-enantiomer,

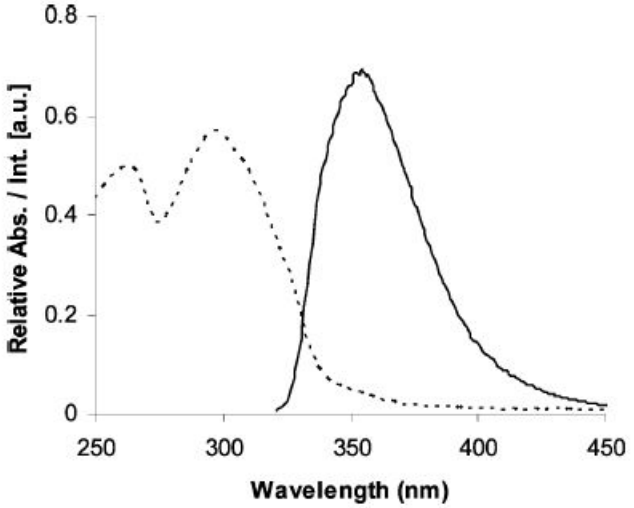

Fig. 2 Emission spectrum (full line) and normalized absorption spectrum (dotted line) of tpy macrocycle **1** in CH_2Cl_2 at room temperature.

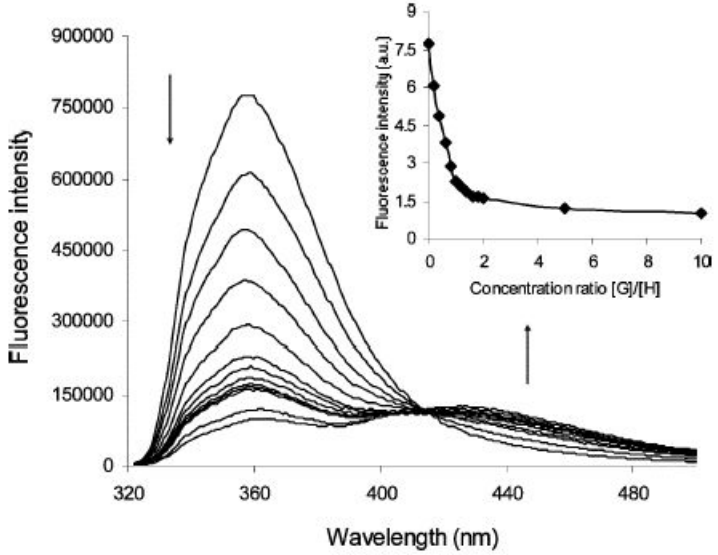

Fig. 3 Fluorometric titration of tpy macrocycle **1** (1.0×10^{-5} M in CH_2Cl_2, λ_{exc} = 316 nm, slit width = 2 nm) with (*S*)-PhEtOMe in CH_2Cl_2 at 25 °C. The insert shows the binding isotherm at 355 nm.

Определение аминокислот

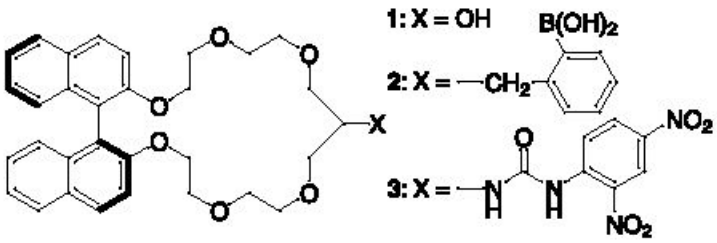

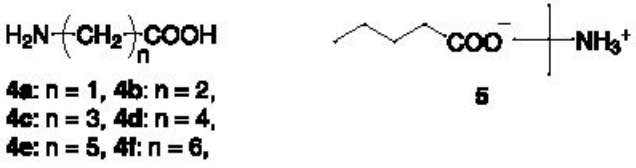

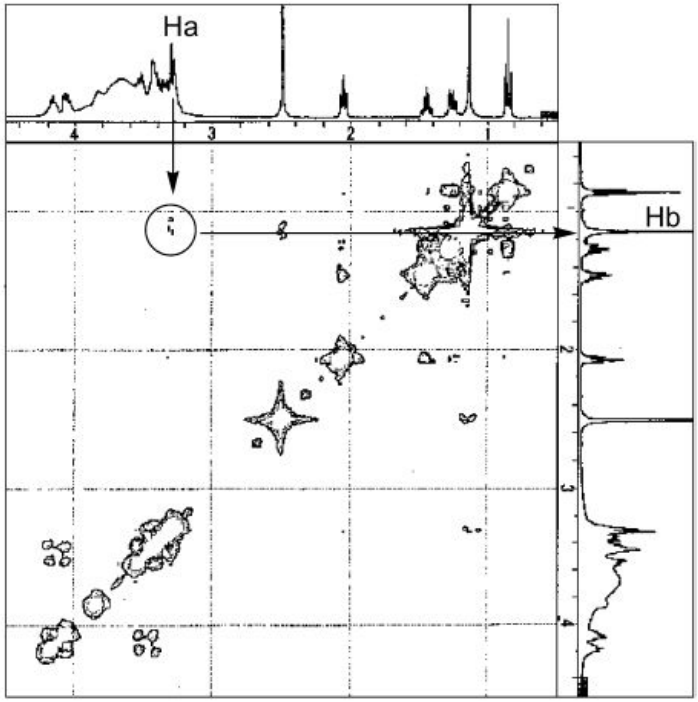

Figure 5. NOESY (400 MHz) spectrum of a 1:1 mixture of Host **3** (1.4×10^{-2} M) and guest **5** in DMSO at 21°C. Ha means the protons of crown ether part of Host **3**, Hb means the *tert*-butyl protons of Guest **5**, respectively.

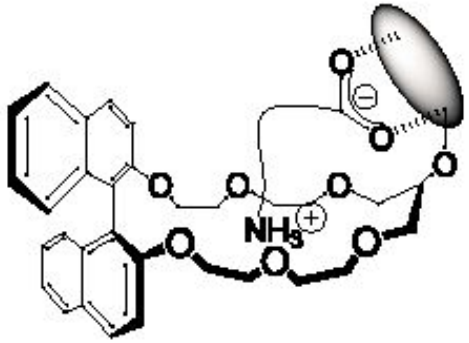

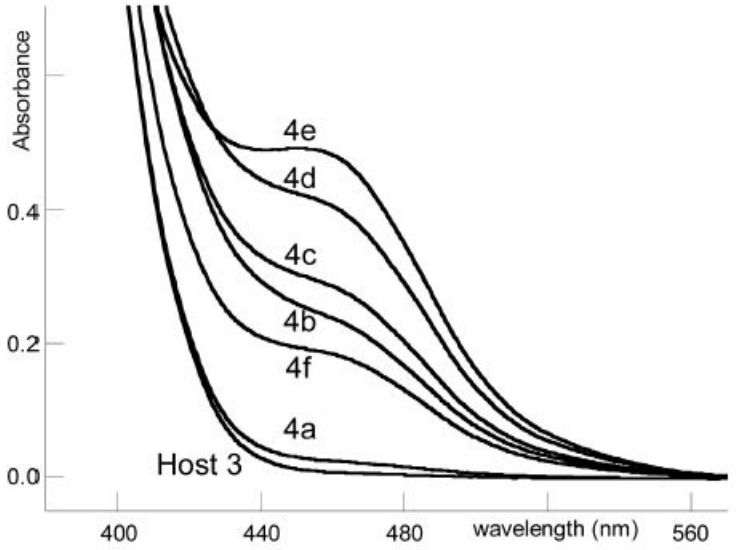

Figure 6. Absorption spectra of after extraction of Guest **4** with Host **3** in DMSO at 20°C. [Host **3**]=5.0×10^{-4} M.

Определение аминокислот

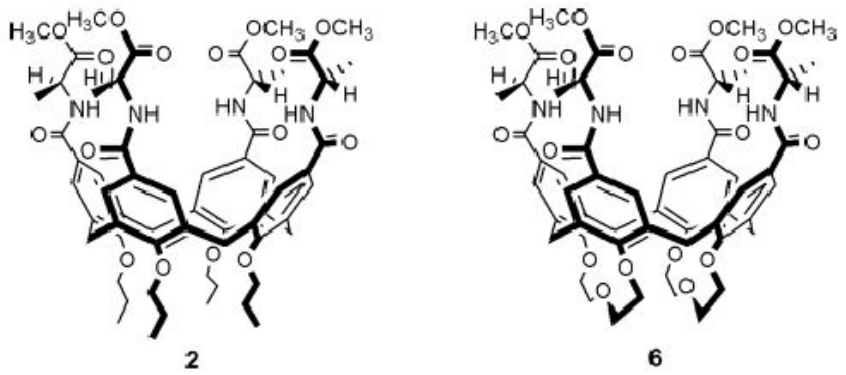

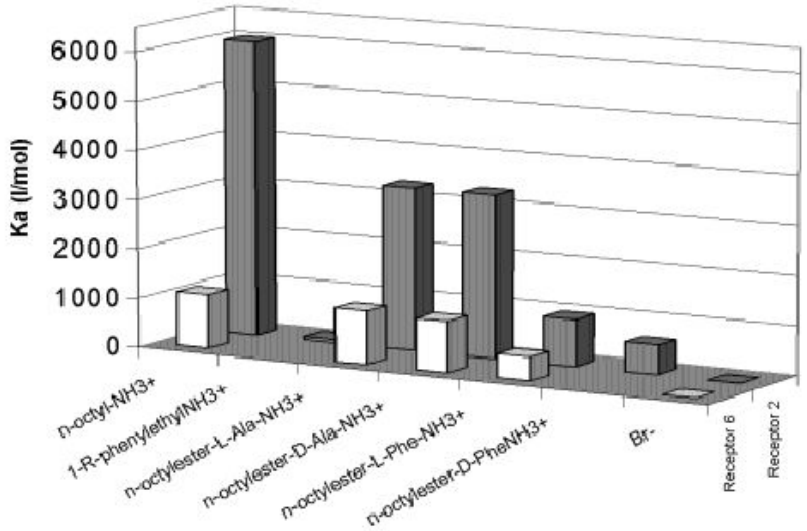

FIGURE 7. Association constants (M^{-1}) with receptors **2** and **6** determined in $CDCl_3$. All ammonium guests were used as bromide salts, except for 1-R-phenylethylammonium, which was used as tetraphenyl borate. Bromide was used as the tetrabutylammonium salt.

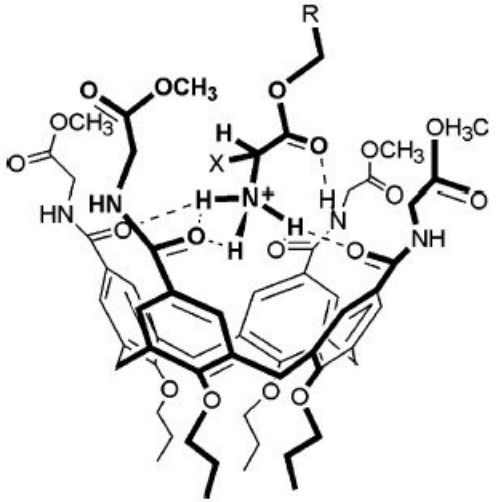

FIGURE 8. Proposed mode of binding of α-amino acid ester derivatives by N-linked tetraalanine methyl ester **2**.

Комплексоны для карбоновых кислот

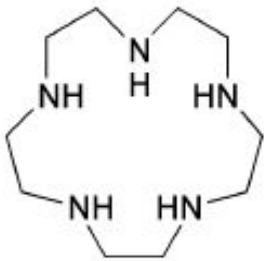

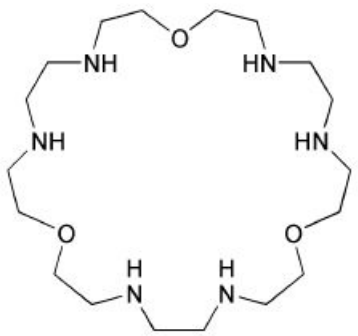

$HO_2CCO_2H > HO_2CCH_2CO_2H > HO_2C(CH_2)_2CO_2H > HO_2CCH{=}CHCO_2H$

щавелевая малоновая янтарная фумаровая кислоты

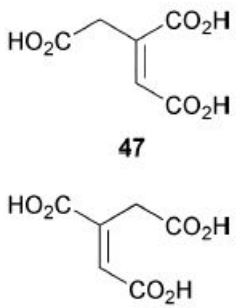

$K_a = 1.3 \cdot 10^5\ M^{-1}$

$K_a = 3.2 \cdot 10^4\ M^{-1}$

Комплексоны для карбоновых кислот

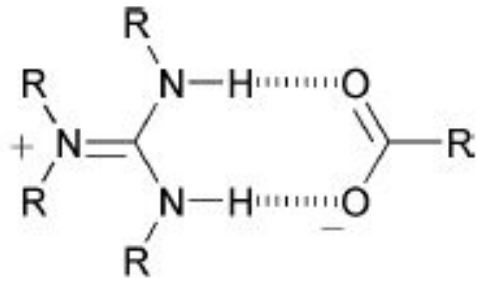

(p*K*a = 13.5, for guanidinium)

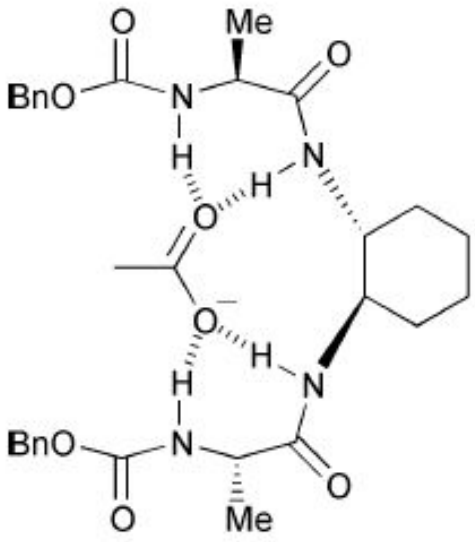

190

*K***a** = 340 M $^{-1}$

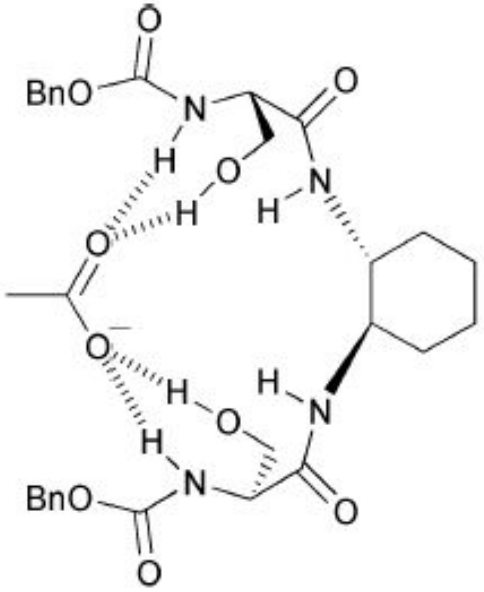

191

*K***a** = 2.8 × 10^{5} M^{-1}

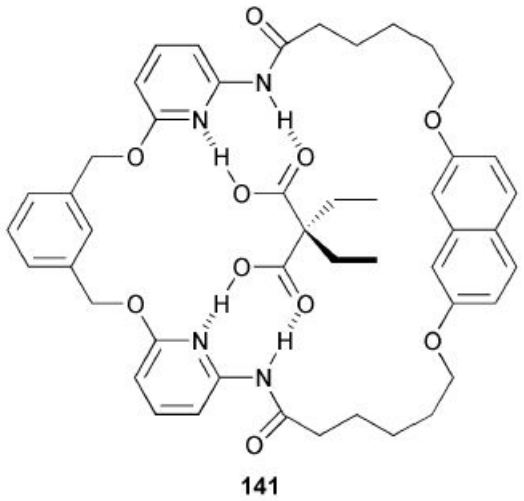

141

*K***a** = 7.3 × 10^{3} M^{-1})

Комплексоны для карбоновых кислот

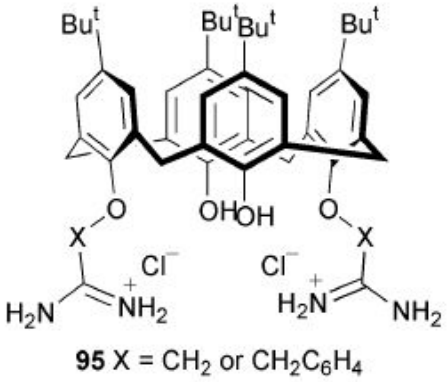

95 X = CH_2 or $CH_2C_6H_4$

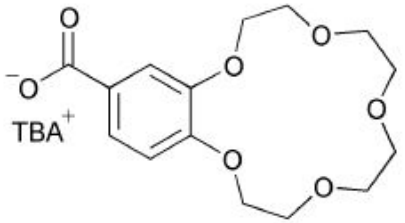

96

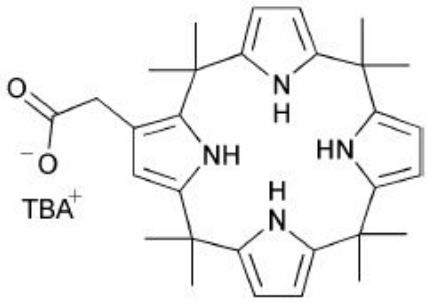

97

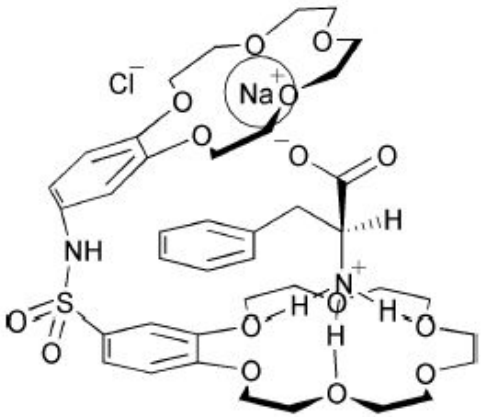

1 : 2 stoichiometry in DMSO.

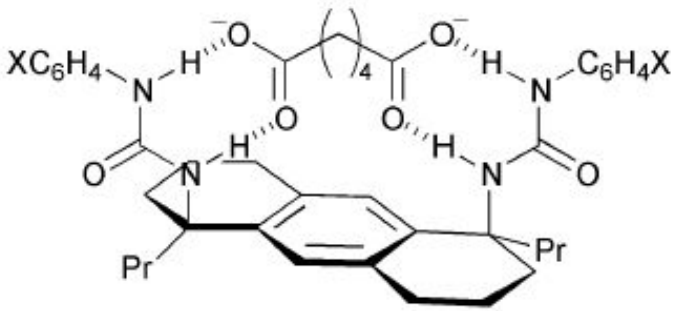

X = NMe_2 K_a = 510 M^{-1},
X = NO_2 K_a = 2.2 . 10^4 M^{-1}

Стереоселективный транспорт аминокислот

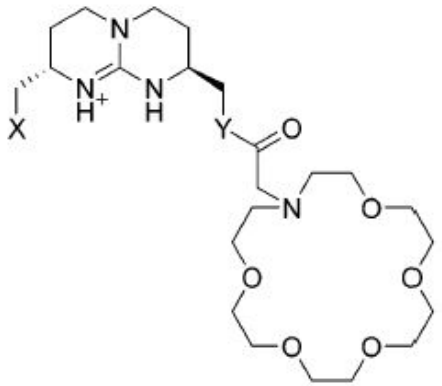

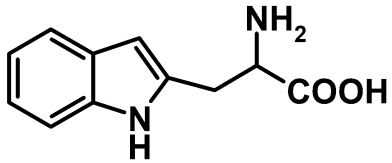

D-, L-

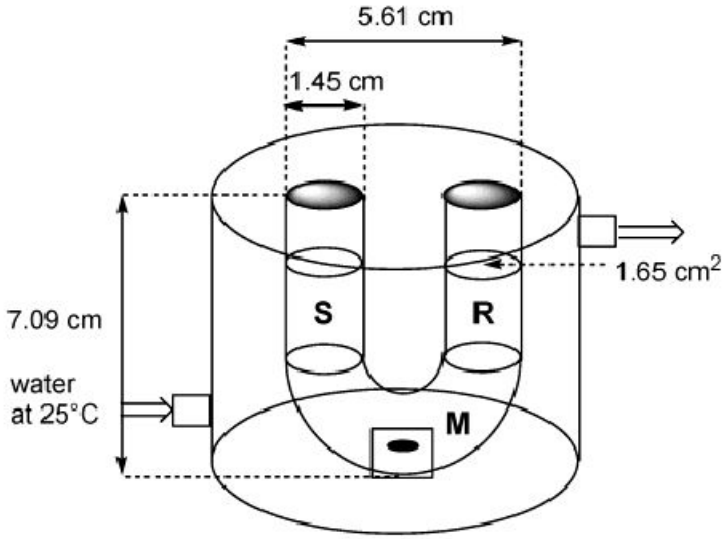

Figure 3. Transport cell.

Table 5. Enantioselectivities in Extraction Experiments

receptor	% ee
1a	75

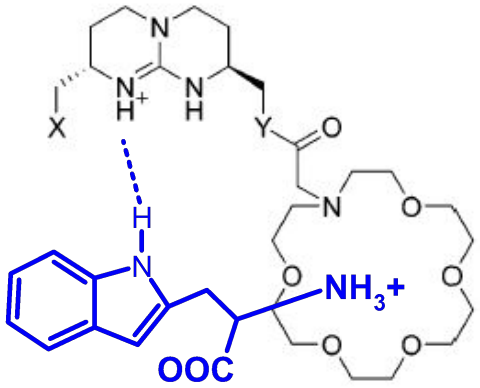

Транспорт допамина через мембрану

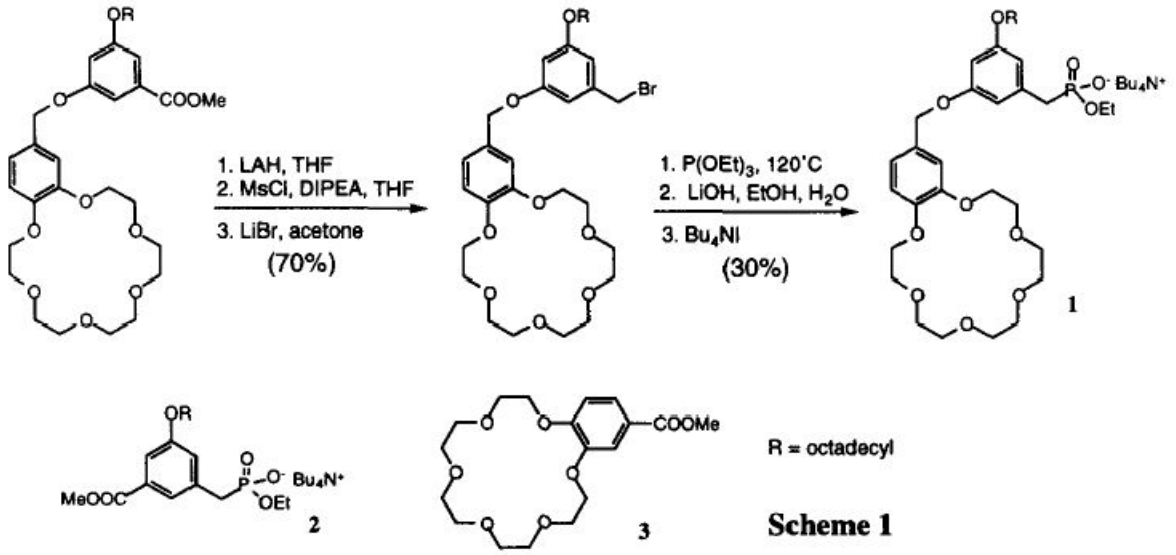

Scheme 1

Table 1. Extraction and Transport of Dopamine by Synthetic Carriers

entry	carrier[a]	extraction (%)[b]	flux (10^{-9} mol/m^2·s)[c]
1	none	3.5	0.76 (1)
2	**1**	41.4	218 (287)
3	**2**	8.1	4.12 (5.4)
4	**3**	9.2	2.54 (3.3)
5	**2 + 3**	10.5	11 (14.5)

[a] Departure phase: sodium phosphate (100 mM, pH 7.4), sodium hydrosulfite (10 mM), and dopamine hydrochloride (41 mM). Organic phase: 1 mM of each carrier in chloroform. Receiving phase: sodium phosphate (100 mM, pH 7.4) and sodium hydrosulfite (10 mM). [b] Aqueous phase: sodium phosphate (100 mM, pH 7.4), sodium hydrosulfite (10 mM), and dopamine hydrochloride (0.3 mM). Organic phase: 3 mM of each carrier in chloroform. [c] Initial transport rate (relative rate in parentheses).

Механизм комплексообразования

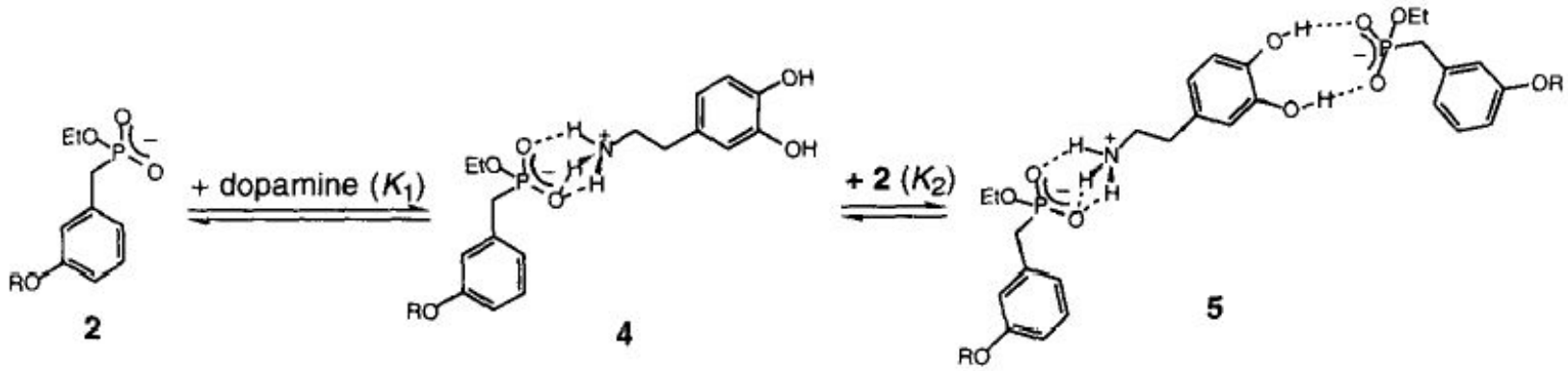

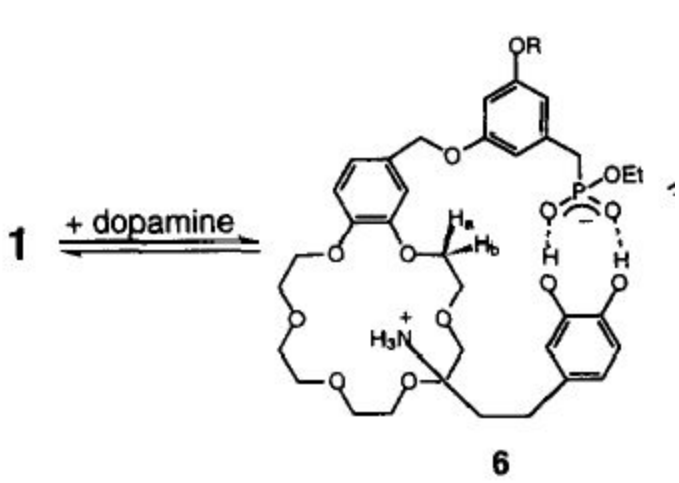

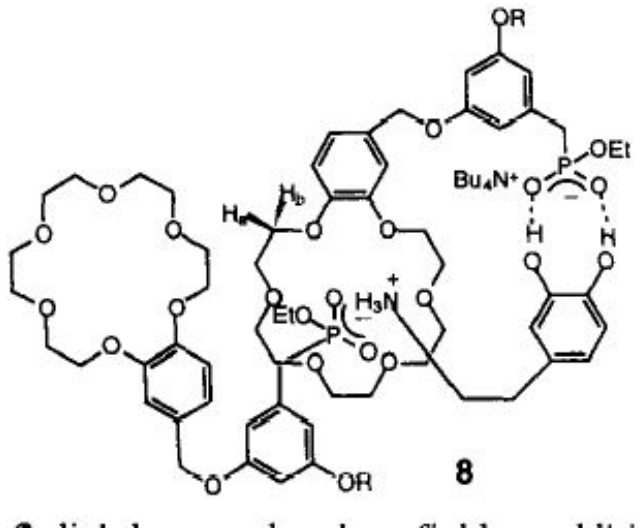

Супрамолекулярный катализ

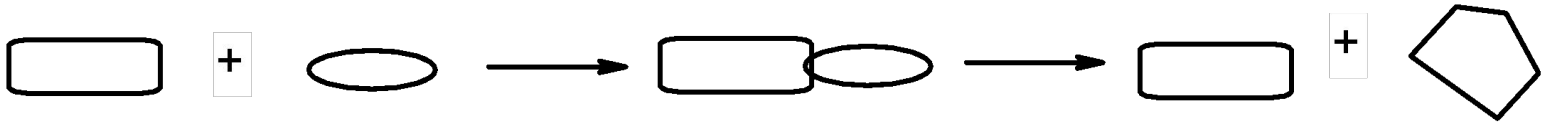

Катализатор Субстрат Супрамолекулярный комплекс Продукт

Супрамолекулярный катализ

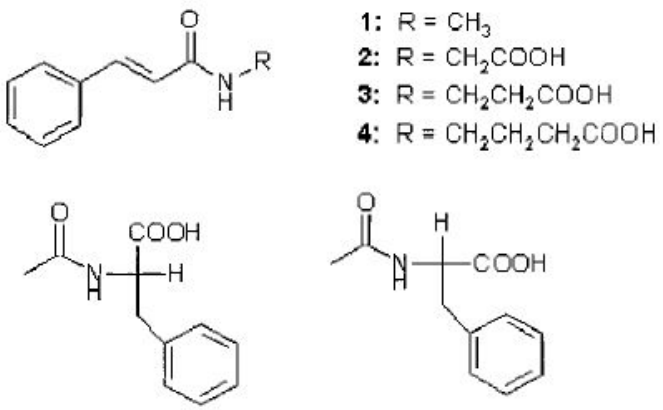

5 (Ac-L-Phe) **6** (Ac-D-Phe)

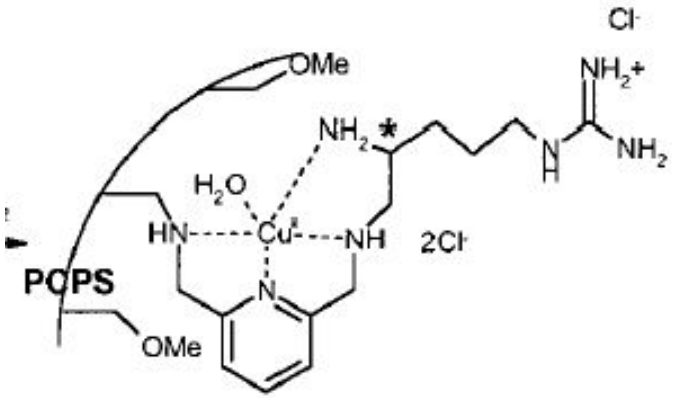

([Cu(II)]Arg^{H}-BAMP)-PCPS^{MeO} **(CABP)**

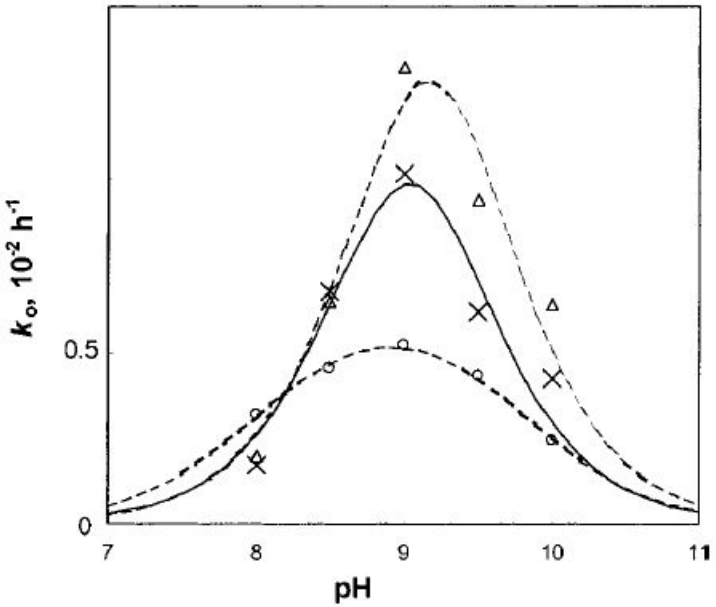

Figure 2. pH dependence of k_0 for hydrolysis of **2** (△), **3** (×), and **4** (○) ($S_0 = 1.96 \times 10^{-4}$ M) promoted by CABP ($C_0 = 1.08$ mM) at 50 °C.

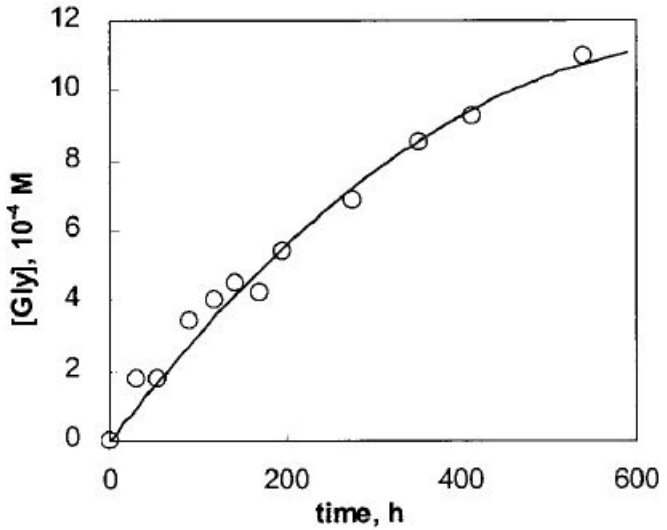

Figure 6. Concentration of Gly released from the hydrolysis of **2** by CABP under the condition of S_0 (2.86 mM) > C_0 (0.394 mM) at pH 9.00 and 50 °C. No reaction occurred in the absence of CABP.

Механизм супрамолекулярного катализа

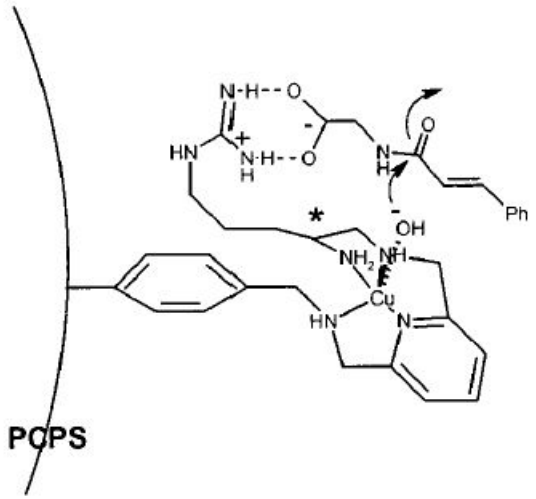

7

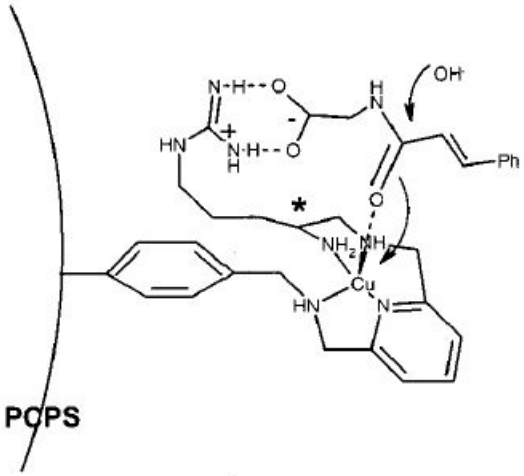

8

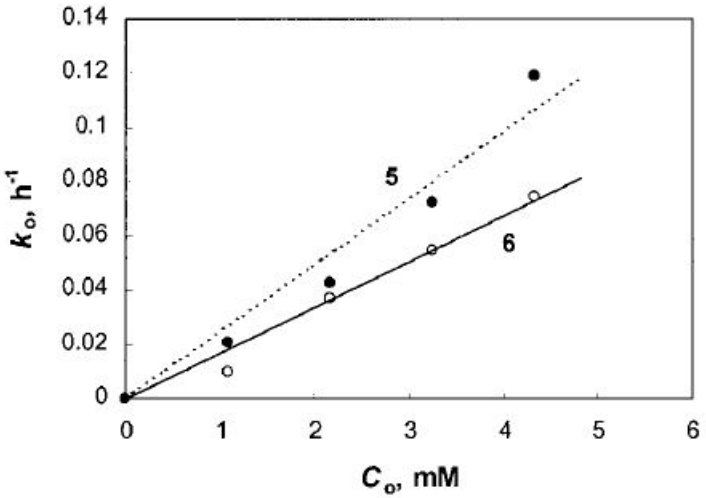

Figure 5. The dependence of k_0 on C_0 for the hydrolysis of **5** and **6** ($S_0 = 1.96 \times 10^{-4}$ M) promoted by CABP at pH 8.50 and 50 °C. Slopes of the straight lines are 24.7 ± 1.6 h^{-1} M^{-1} for **5** and 16.9 ± 0.7 h^{-1} M^{-1} for **6**.

Супрамолекулярный катализ

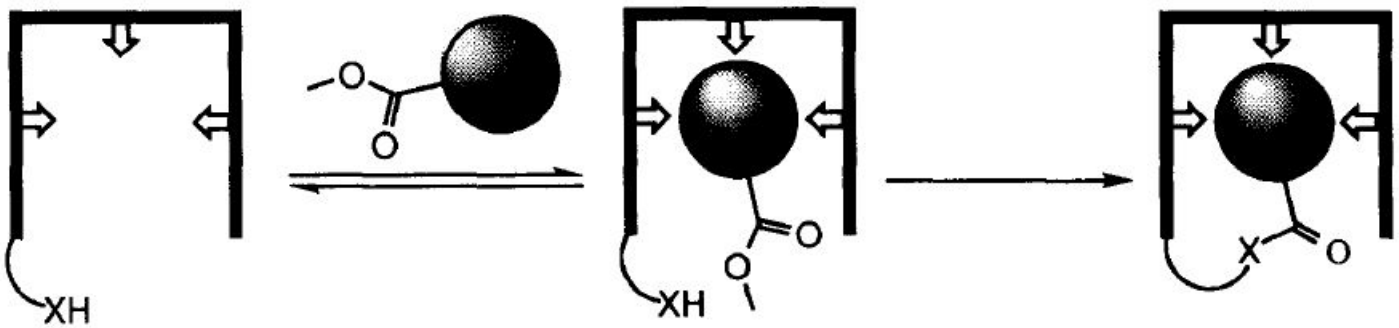

Figure 1. Schematic design of transacylase mimics.

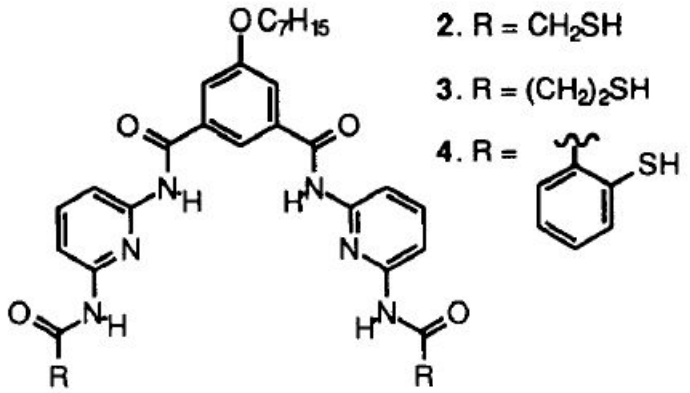

2. R = CH_2SH

3. R = $(CH_2)_2SH$

4. R =

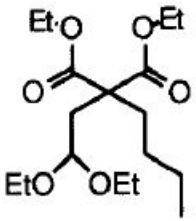

6

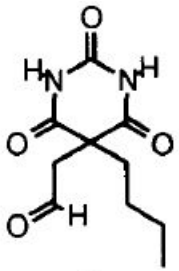

7

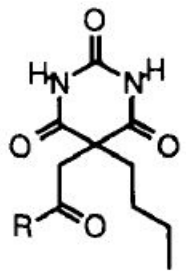

8a. R = OH

8b. R = 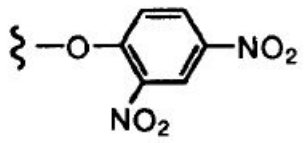

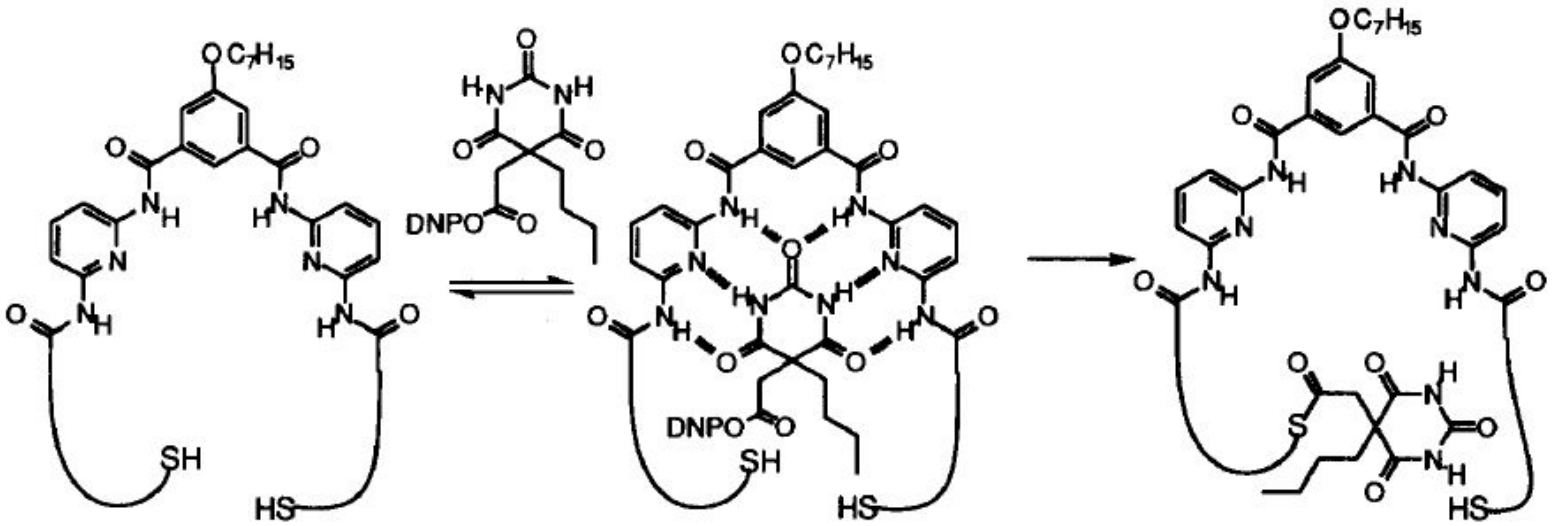

Figure 2. Receptor mediated thiolysis reaction.

Table 1. Pseudo-first order rate constants for reaction of **8b** with thiomethyl derivatives.

Catalyst	[Cat] x 10^4 (M)	[Cat]/[8b]	k_{obs} (sec^{-1})	k_{obs}/k_o
$HSCH_2CO_2Et$	4.64	21	6.40×10^{-6}	1
9	4.64	21	3.91×10^{-5}	61
2	2.42	11	1.41×10^{-3}	220
2	2.90	13	1.67×10^{-3}	260
2	3.39	15	1.83×10^{-3}	285
2	3.88	17.4	1.94×10^{-3}	300
2	4.36	19.5	2.15×10^{-3}	335

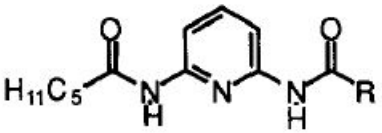

9. R = CH_2SH **10**. R =

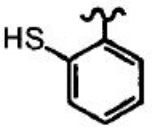

Фотоуправляемый этанолиз

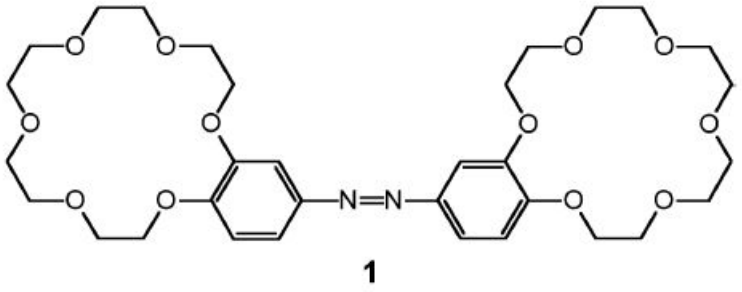

1

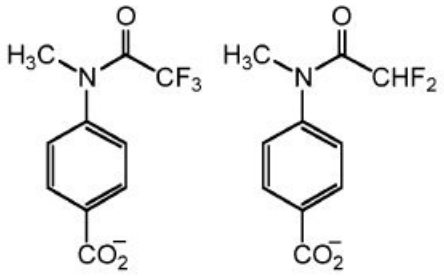

2 3

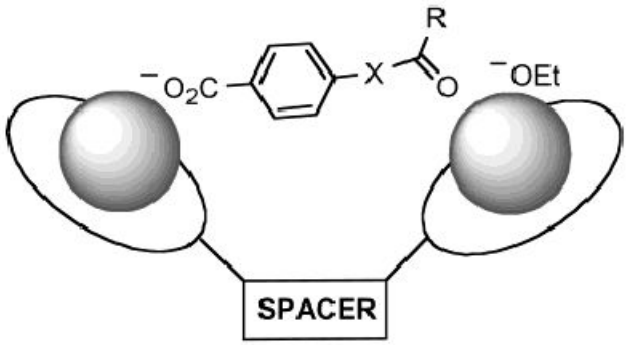

X = N(Me), O

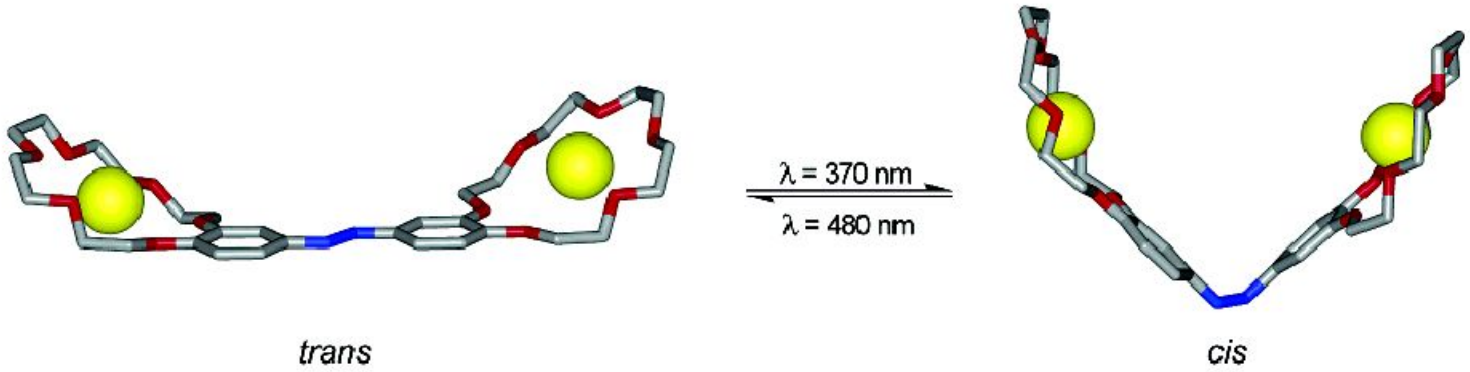

Figure 4. Computer-generated structures of interswitchable trans and cis forms of **1**·$[Ba]_2$.

Table 1. Catalysis of the Basic Ethanolysis of Anilides **2** and **3** in EtOH−CH_3CN (65/35 v/v) at 25 °C[a]

substrate	additive (0.10 mM)	k_{obs}[b] (s^{-1})	k_{rel}
2	none	3.93×10^{-5}	1
	trans-**1**·$[Ba]_2$	1.09×10^{-2}	280
	quasi-*trans*-**1**·$[Ba]_2$	1.84×10^{-2}	470
	quasi-*cis*-**1**·$[Ba]_2$	4.89×10^{-2}	1240
3	none	1.85×10^{-6}	1
	trans-**1**·$[Ba]_2$	4.26×10^{-4}	230
	quasi-*trans*-**1**·$[Ba]_2$	7.82×10^{-4}	420
	quasi-*cis*-**1**·$[Ba]_2$	2.36×10^{-3}	1280

[a] Experiments carried out on 0.025 mM substrate solutions in the presence of 1.00 mM Me_4NOEt. [b] Clean first-order time dependence was observed in all cases. Error limits are on the order of ±5%.

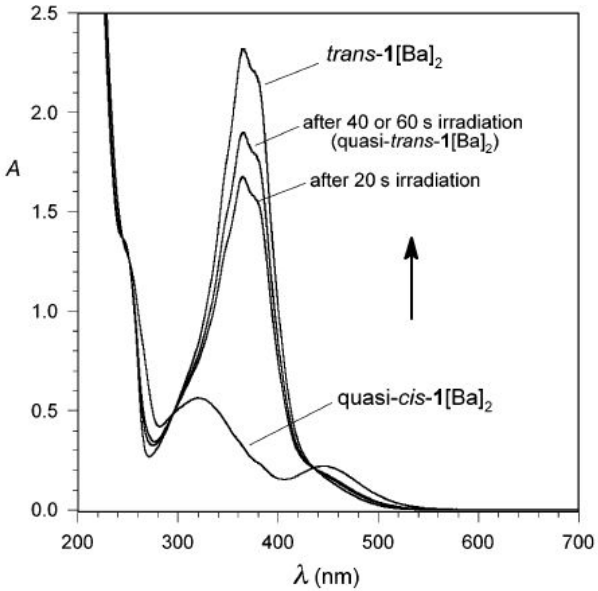

Figure 3. UV−vis spectra of 0.10 mM quasi-*cis*-**1**·$[Ba]_2$ before and after irradiation at 480 nm. The spectrum of 0.10 mM *trans*-**1**·$[Ba]_2$ is shown for comparison.

Гидролиз АТФ

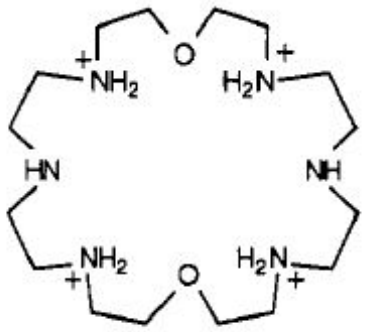

1

Scheme I

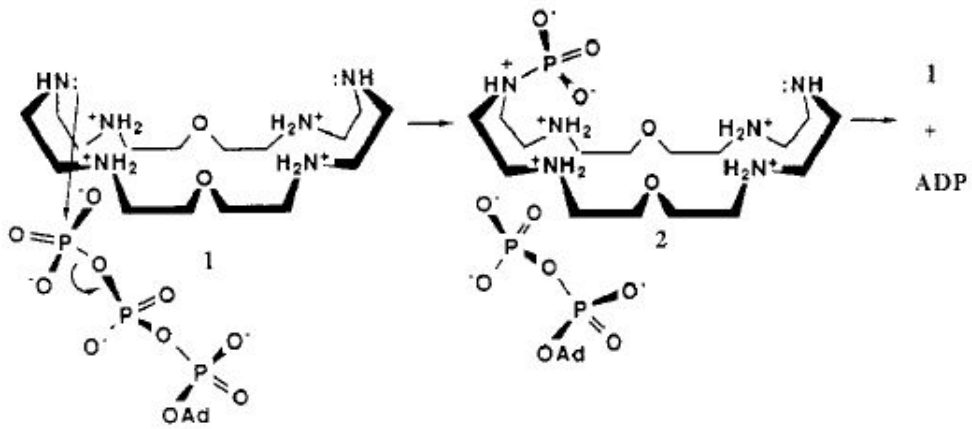

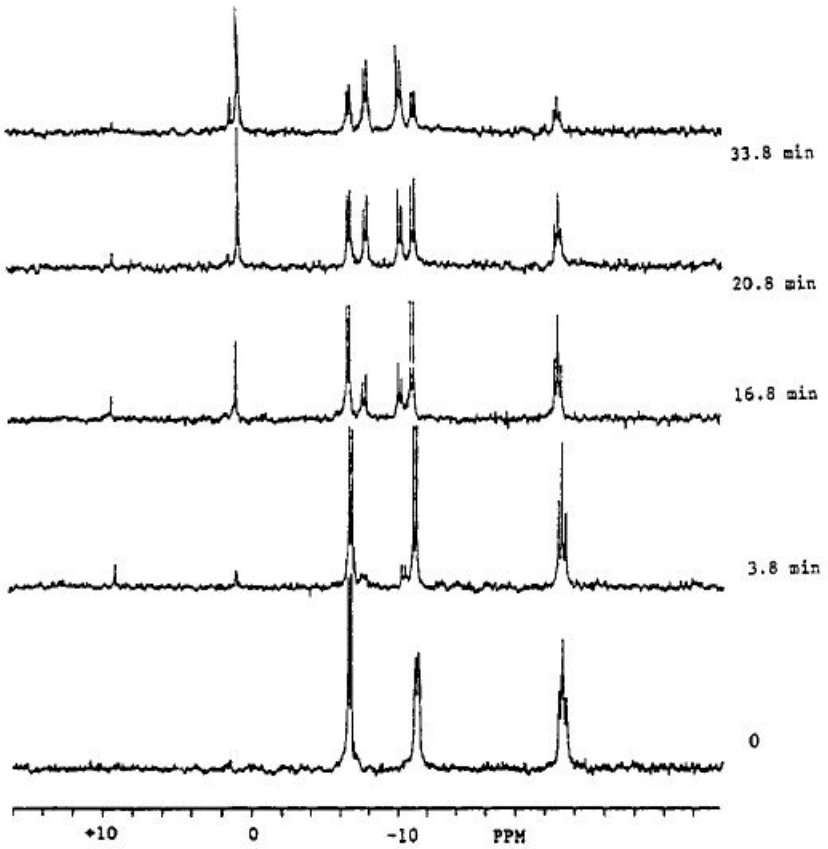

Figure 1. ^{31}P NMR spectra of ATP and [24]N_6O_2 (1) (0.03 M in each) in 10% D_2O/H_2O at pH 7.0 and 70 °C. The chemical shift assignments: ATP, $\alpha = -10.6$, $\beta = -20.6$, $\gamma = -5.7$; ADP, $\alpha = -9.2$, $\beta = -6.0$; inorganic phosphate (P_i), +2.5; AMP, +3.3; phosphoramidate, +10.3 ppm. The chemical shifts are relative to 0 ppm for 85% H_3PO_4 as an external standard (+, downfield).

Гидролиз АТФ

Table II
Comparison of ATPase- and Macrocycle-Catalyzed Dephosphorylation of ATP Using Lineweaver–Burk Kinetics

catalyst	K_m, M	V_m, μM/min	k_{cat}, min^{-1}	k_{cat}/K_m
none			2.5×10^{-4}	
ATPase	1×10^{-4}		3.2×10^{4}	3.2×10^{8}
1	1×10^{-4}	0.064	6.4×10^{-2}	6.4×10^{2}

Properties of ATPases

$$ATP + H_2O \xrightarrow{ATPase/Mg^{2+}} ADP + P_1$$

Гидролиз динуклеотида

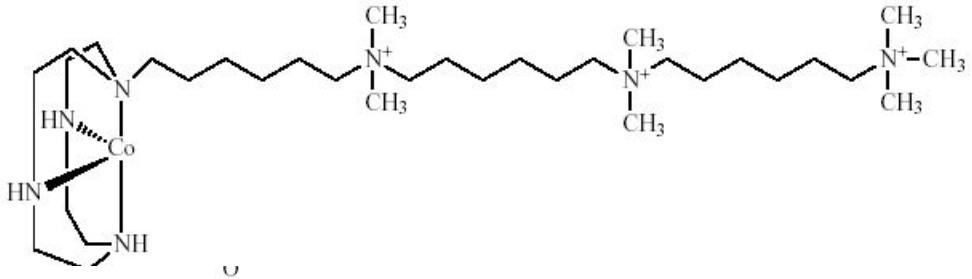

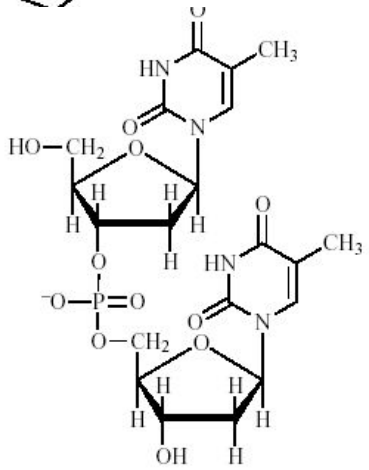

TpT

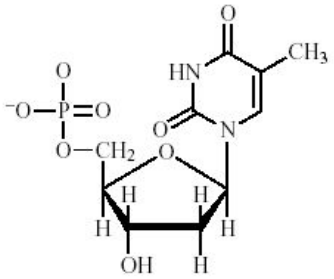

5′-TMP

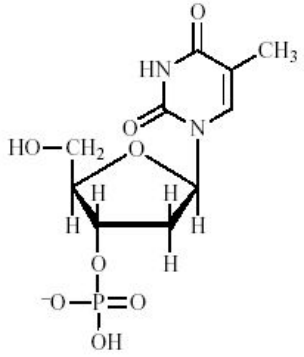

3′-TMP

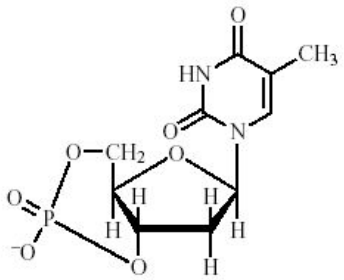

3′, 5′-cTMP

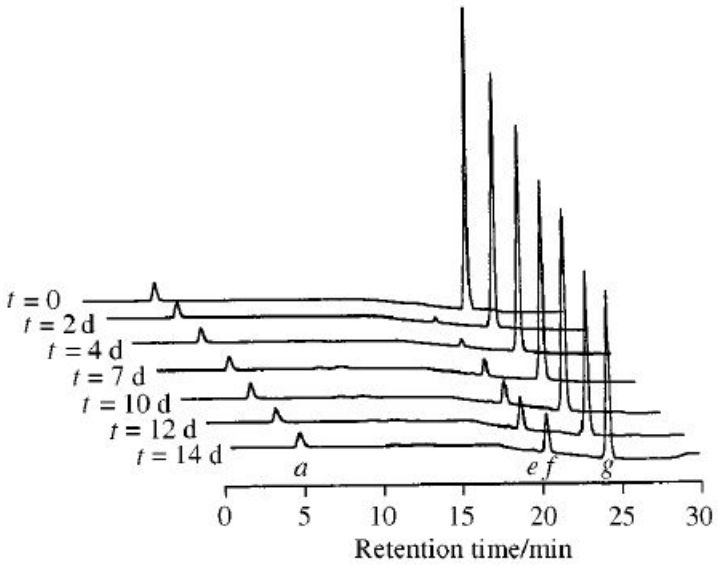

Комплексоны для биологических молекул

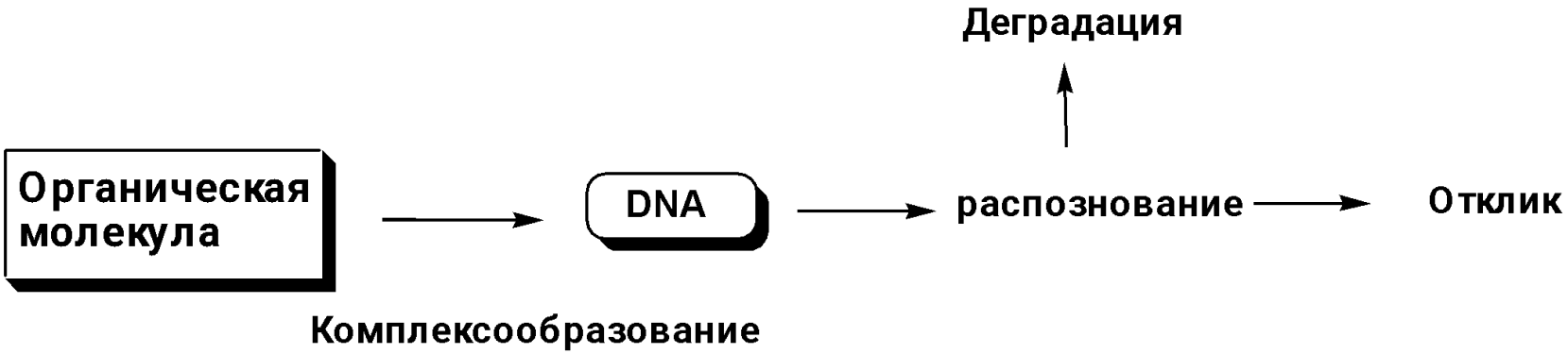

Комплексоны для биологических молекул

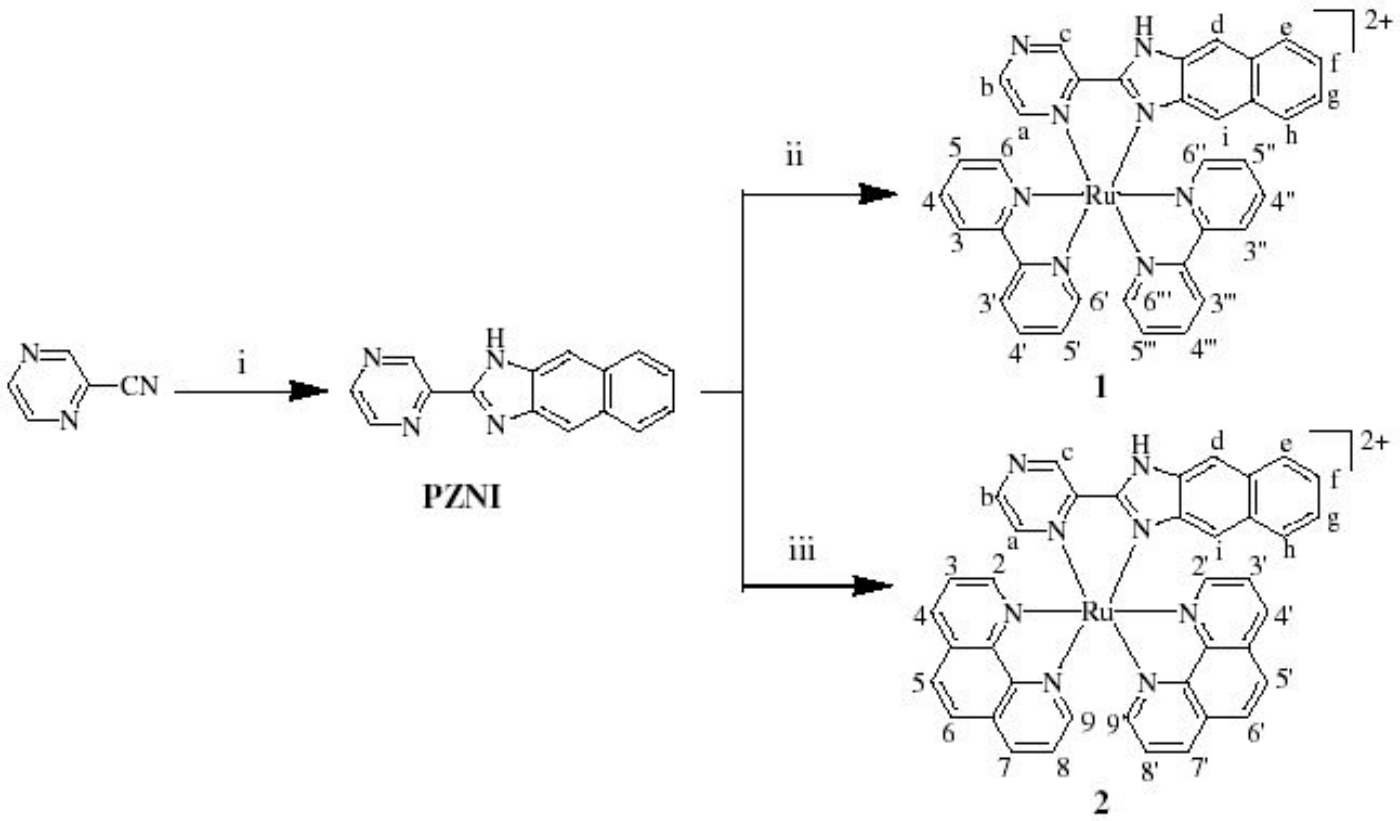

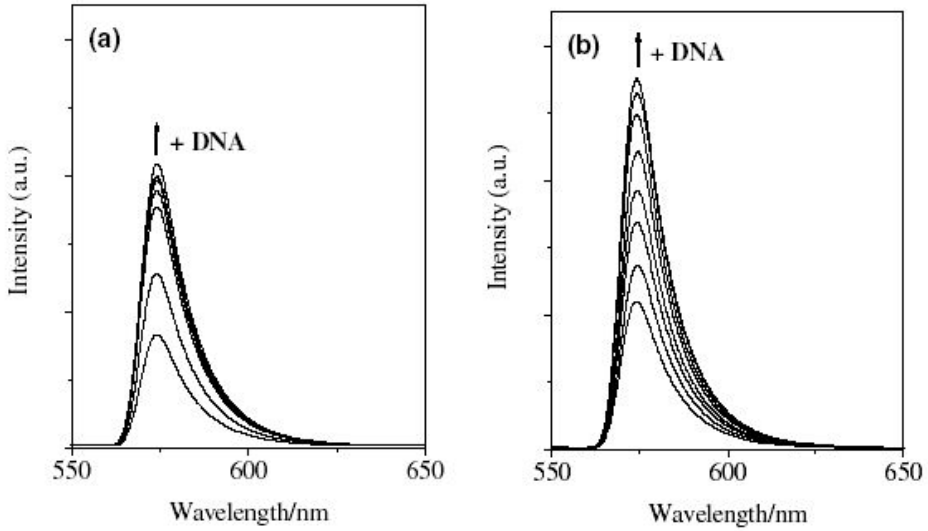

Fig. 2. Emission spectra of complexes **1** (a) and **2** (b) in Tris–HCl buffer in the absence and presence of CT DNA. Arrow shows the intensity change upon increasing DNA concentrations.

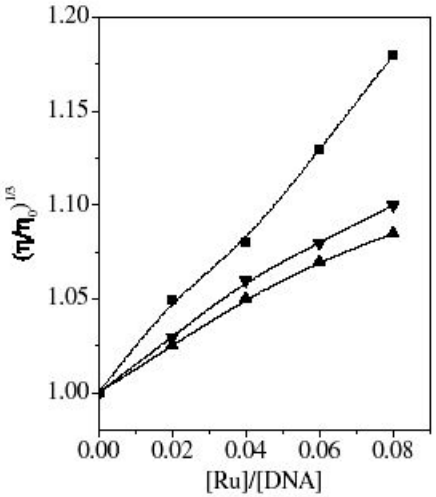

Fig. 4. Effect of increasing amounts of $[Ru(bpy)_2\ (dppz)]^{2+}$ (■), complex **1** (▲) and complex **2** (▼) on the relative viscosity of calf thymus DNA at 28 (±0.1) °C. The total concentration of DNA is 0.5 mM.

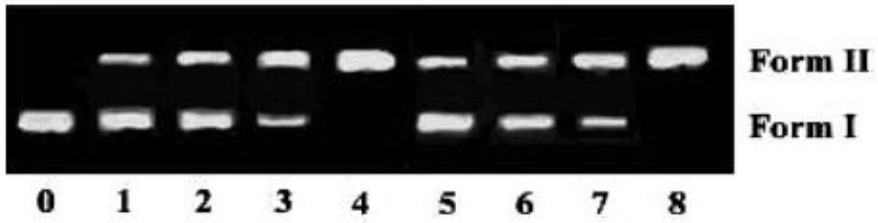

Fig. 5. Photoactivated cleavage of pBR 322 DNA in the presence of Ru(II) complexes, light after 60 min irradiation at 365 nm. Lane 0, DNA alone; lanes 1–4, in the different concentrations of complex **1**: (1) 20; (2) 40; (3) 60; (4) 80 μM; lanes 5–8, in the different concentrations of complex **2**: (1) 20; (2) 40; (3) 60; (4) 80 μM.

Комплексоны для биологических молекул

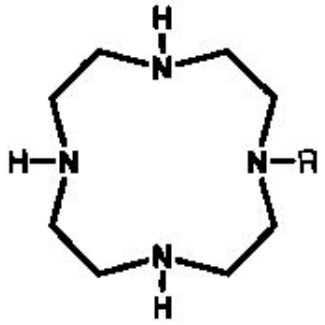

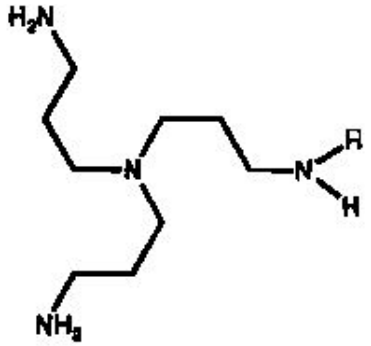

1 R = H *(Cyclen)*

3 R = (CH2)3-N+(CH3)3

4 R = (CH2)4-N+(CH3)3

5 R = (CH2)5-N+(CH3)3

6 R = (CH2)6-N+(CH3)3

7 R = (CH2)6-N+(CH3)2-(CH2)6-N+(CH3)3

8 R = [(CH2)6-N+(CH3)2]3-CH3

10 R = [(CH2)6-N+(CH3)2]2-(CH2)6-Cyclen

2 R = H *(Trpn)*

9 R = (CH2)6-N+(CH3)3

11 R = [(CH2)6-N+(CH3)2]2-(CH2)6-Trpn

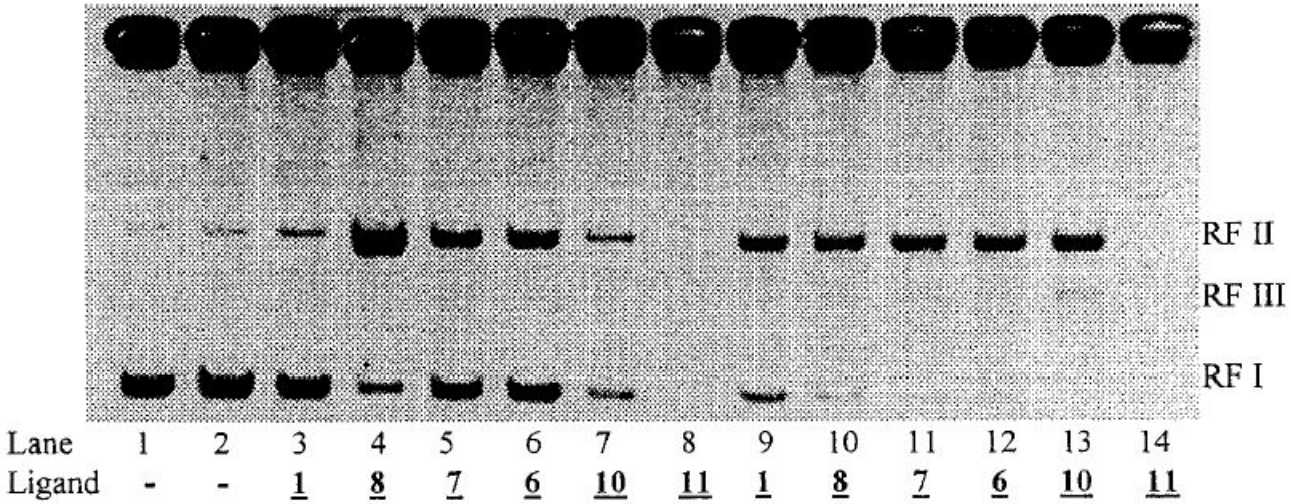

Figure 4. Electrophoretic separations of DNA cleavage with copper(II) complexes (lanes 3−8: [1×10^{-4} M]; lanes 9−14: [1×10^{-6} M] in presence of H_2O_2 [1×10^{-4} M] and ascorbic acid [1×10^{-4} M].

Table 7. DNA Cleavage with Copper Complexes in Presence of H_2O_2 and Ascorbic Acid[a]

lane	Cu^{2+} complex of compd	concn [M]	H_2O_2 [1×10^{-4} M]	ascorbate [1×10^{-4} M]	RF I [%]
1			−	−	100
2			+	−	99.5
3	1	1×10^{-4}	+	−	91.5
4	8	1×10^{-4}	+	−	33.0
5	7	1×10^{-4}	+	−	44.4
6	6	1×10^{-4}	+	−	59.8
7	10	5×10^{-4}	+	−	60.4
8	11	5×10^{-4}	+	−	
9	1	1×10^{-6}	+	+	37.2
10	8	1×10^{-6}	+	+	4.3
11	7	1×10^{-6}	+	+	4.9
12	6	1×10^{-6}	+	+	2.9
13	10	5×10^{-7}	+	+	5.3
14	11	5×10^{-7}	+	+	

Комплексоны для биологических молекул

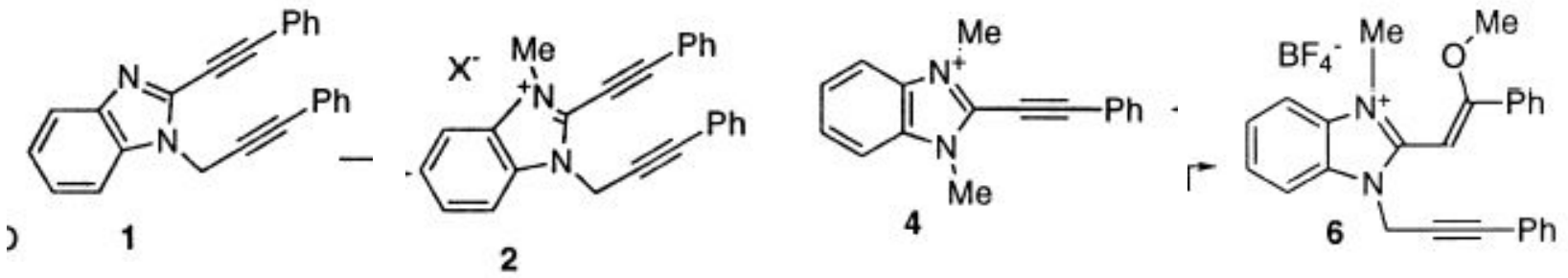

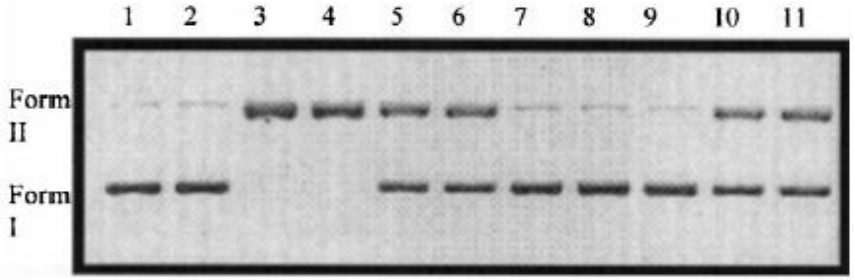

Figure 2. DNA cleavage by **2**. pBR322 plasmid DNA (50 μM base pairs) was incubated with various concentrations of **2** (pH 8, 50 mM Tris buffer, 13% v/v DMSO, 20 h at 37 °C) and analyzed by gel electrophoresis (0.8% agarose, ethidium bromide stain). Lanes 1, 2, and 9, DNA without drug; lanes 3–4, 1 mM **2**; lanes 5–6 and 10–11, 100 μM **2**; lane 7, 10 μM **2**; lane 8, 1 μM **2**; lanes 9, 10, and 11 were heated at 70 °C for 90 s after incubation.

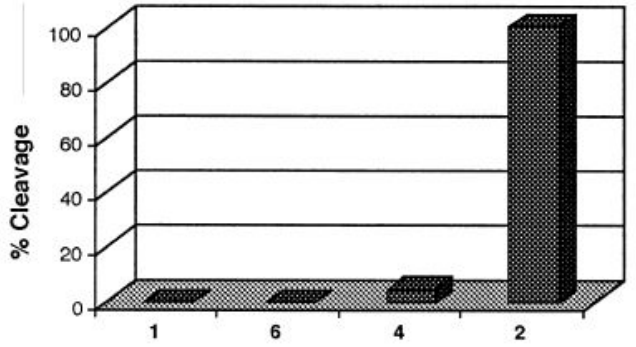

Figure 3. DNA cleavage by **1**, **6**, **4**, and **2**. ΦX174 (RF-1) phage DNA (50 μM base pairs) was incubated with 1 mM **1**, **6**, **4**, or **2** (pH 8, 50 mM Tris buffer, 13% v/v DMSO, 20 h at 37 °C) and analyzed by gel electrophoresis (0.8% agarose, ethidium bromide stain).